Interference effects with surface plasmons

Kuzmin, N.V.

Chapter 1

Introduction

1.1 Basic properties of metals

Since ancient times people have been intrigued by the sparkling properties of crystals and the shimmering of shiny metals like gold and silver. These precious metals were valued by many cultures and used as coinage, for ornaments and jewelry.

Polished silver surfaces were also used as mirrors and legend has it that, during the second Punic war, Archimedes used a large number of mirrors to set afire a hostile Roman fleet anchored off the bay of Syracuse, by focusing the light of the sun on the ships [1, 2]. Gold was also used to make stained glass, well known from the windows of many cathedrals around Europe and, much earlier, to make the base glass of the well-known Lycurgus cup [3]. An understanding of the physics of these phenomena came much later, in the 19^{th} and 20^{th} centuries, when scientists came up with a theoretical description of the optics of metals.

In one of these models, the so-called free-electron model, a metal is described as a collection of ions, that are fixed in space, and a gas of free conduction electrons that interact with themselves and with the ions through the Coulomb force [4, 5]. The interacting system of ions and electrons is basically a plasma where the ions have much larger inertia than the electrons. When this plasma interacts with an electromagnetic field, the electrons will execute a forced oscillation relative to the ions. The amplitude and phase of this oscillation relative to that of the driving electromagnetic field depends on the frequency of the latter relative to the eigen oscillation frequency of the plasma, the so-called *plasma frequency* ω_{p}:

$$\omega_{\text{p}}^2 = \frac{ne^2}{\epsilon_0 m^*}, \tag{1.1}$$

which follows directly from a simple harmonic oscillator description of the response of the electrons [4]. Here n is the electron density, e and m^* are the charge and effective mass of the electron. The quantum of this oscillation is called a *plasmon*, or, since the electrons are oscillating in the metal volume, a *bulk plasmon*. For gold and silver $\omega_\mathrm{p} \sim 10^{16}$ rad/s.

The plasma oscillation is damped, for instance, due to the scattering of the electrons off impurities, lattice defects, etc. Phenomenologically, this is taken into account by introducing a damping constant γ, and in the Drude model [4] the relative dielectric function is expressed as:

$$\tilde{\epsilon}(\omega) = 1 - \frac{\omega_\mathrm{p}^2}{\omega(\omega + i\gamma)}. \tag{1.2}$$

Here γ represents the collision rate of the electrons and determines the damping of the plasma oscillation. The Drude model is a simple and convenient model that explains, for instance, the high reflectivity of metals in the visible and infrared, i.e. below the plasma frequency. In that spectral regime the real part of the dielectric function is negative $\epsilon'(\omega) \equiv \mathrm{Re}(\tilde{\epsilon}) < 0$ and the incident electromagnetic radiation is back reflected by the plasma, penetrating into the metal only over a distance of the order of $\lambda/2\pi\sqrt{|\epsilon'_\mathrm{m}|}$, which is $\simeq 25$ nm for case of gold at $\lambda = 0.8$ μm. In the UV range, i.e., above the plasma frequency, $\epsilon'(\omega)$ is positive and the metal is transparent for incident electromagnetic radiation.

1.2 Surface plasmons

In 1957 Ritchie theoretically showed [6] that, when a metal is in the form of a thin foil, a second type of plasma resonance can occur at $\omega = \omega_\mathrm{p}/\sqrt{2}$. Here the charge oscillations take place at the top and bottom interfaces of the metal film. This prediction was confirmed in an experiment by Powell and Swan [7].

1.2.1 What is a surface plasmon?

This collective oscillation of the electron gas on the interface between a metal and a dielectric has become known as the *surface plasmon* (SP). Theoretically, surface plasmons simply arise as a purely 2D solution of Maxwell's equations that propagates as a transverse magnetic wave along the metallo-dielectric interface [8]. This wave is evanescent in both the dielectric and the metal. This characteristic nature of the surface plasmon follows from the requirement that the interface is "active", i.e., that the real parts of the dielectric functions $\epsilon'(\omega)$ of the media on either side of the interface have opposite signs.

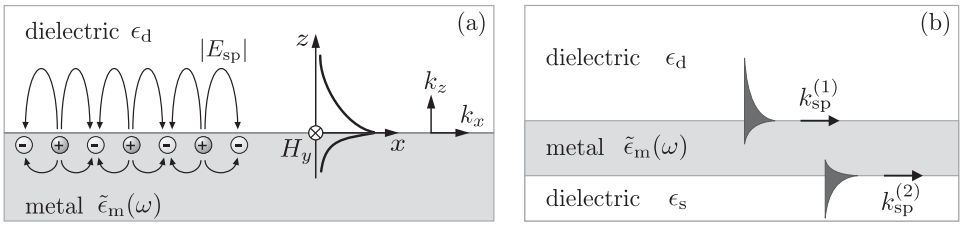

Figure 1.1. (a) Schematic picture of the charge distribution of a surface plasmon and the associated electromagnetic wave. (b) Metal film, sandwiched between two dielectrics, carrying surface plasmons at each interface. When the metal film is thin ($\lesssim 50$ nm) the plasmons of both interfaces can couple via their evanescent fields.

In the recent literature [9] a distinction is made between surface plasmons, that *propagate* on essentially extended interfaces (length scale much larger than the optical wavelength), called *surface-plasmon polaritons*, and *localized* surface plasmons which are associated with metal objects or protrusions that are much smaller than the wavelength [10, 11]. The latter are referred to as "particle plasmons" and are responsible, e.g., for the optical properties of the Lycurgus cup mentioned earlier.

The boundary conditions for the electromagnetic field require that the magnetic field of a surface plasmon, propagating along a smooth and flat interface, is parallel to the metal surface. With the SP, propagating in the x-direction as a transverse magnetic wave, we have $H_x = H_z = 0$. The propagation constant of the SP is complex:

$$\tilde{k}_x \equiv k_\mathrm{sp} + ik_x'' = \frac{\omega}{c}\sqrt{\frac{\tilde{\epsilon}_\mathrm{m}\epsilon_\mathrm{d}}{\tilde{\epsilon}_\mathrm{m}+\epsilon_\mathrm{d}}}, \tag{1.3}$$

with $\tilde{\epsilon}_\mathrm{m}$ and ϵ_d the dielectric functions of the metal and of the dielectric, respectively. Note that $\tilde{\epsilon}_\mathrm{m}$ is complex: $\tilde{\epsilon}_\mathrm{m} = \epsilon_\mathrm{m}' + i\epsilon_\mathrm{m}''$ with $\epsilon_\mathrm{m}' < 0$.

The magnetic component of the surface-plasmon field can be written as

$$\vec{H}_\mathrm{sp} = \hat{y}\, H_y\, f(z)\, \exp[i(\tilde{k}_x x - \omega t)], \tag{1.4}$$

with

$$f(z) = \begin{cases} \exp(-q_\mathrm{d} z) & \text{for } z > 0, \\ \exp(+q_\mathrm{m} z) & \text{for } z < 0, \end{cases} \tag{1.5}$$

where $\tilde{k}_x^2 - q_i^2 = \epsilon_{\rm i}(\omega/c)^2$, $i = {\rm m}, {\rm d}$. In the limit that $|\epsilon'_{\rm m}| \gg \epsilon_{\rm d}$ one has

$$\begin{aligned} q_{\rm d} &\simeq \frac{\omega}{c}\,\frac{\epsilon_{\rm d}}{\sqrt{|\epsilon'_{\rm m}|}}, \\ q_{\rm m} &\simeq \frac{\omega}{c}\,\sqrt{|\epsilon'_{\rm m}|}, \end{aligned} \tag{1.6}$$

showing that the surface plasmon field decays in the z-direction over a length roughly equal to $\lambda\sqrt{|\epsilon'_{\rm m}|}/2\pi\epsilon_{\rm d}$ in the dielectric and $\lambda/2\pi\sqrt{|\epsilon'_{\rm m}|}$ in the metal. For large values of $|\epsilon'_{\rm m}|$ the field extends well into the dielectric (microns) and only marginally into the metal (nanometers). The fact that the electromagnetic field of a surface plasmon is confined to the metallo-dielectric interface makes SP into a highly sensitive probe of such interfaces [12, 13].

The electric field of the surface plasmon has both a longitudinal (x) and transverse (z) components with ratio

$$\begin{aligned} \frac{E_x}{E_z} &= -i\,\frac{q_{\rm d}}{k_{\rm sp}} \quad \text{for } z > 0, \\ \frac{E_x}{E_z} &= +i\,\frac{q_{\rm m}}{k_{\rm sp}} \quad \text{for } z < 0, \end{aligned} \tag{1.7}$$

so that fields in both media are "elliptically" polarized.

An important property of the surface plasmon is that it is attenuated during propagation, basically due to dissipation in the metal — the electrons are inelastically scattered. The field attenuation length, i.e. the length over which the SP field amplitude decays by factor e in the x direction, is given by $L_{\rm sp} = 1/k''_x$. For gold and silver $L_{\rm sp}$ spans from millimeters in the mid-infrared range to less than a micron in the blue part of the visible spectrum (see Fig. 1.3b). A second cause of surface plasmon damping is surface roughness [8, 14].

When the metal does not form a half space, but is shaped as a thin film on top of a dielectric, surface plasmons can propagate along both interfaces of that film (see Fig.1.1b), and, if the film is sufficiently thin, i.e., $\lesssim 50$ nm, these SPs can couple [15]. For a symmetrically-embedded metal film the interaction between the evanescent SP fields in the metal gives rise to symmetric and asymmetric modes, which have very different attenuation lengths [16]. The asymmetric mode can propagate for a much longer distance than its symmetric counterpart, and its propagation length is considerably larger than that of a plasmon on a semi-infinite interface. The SPs with long propagation length are called *long-range surface plasmons* [17]. In the present thesis, however, the focus is on surface plasmons propagating along a *single* interface.

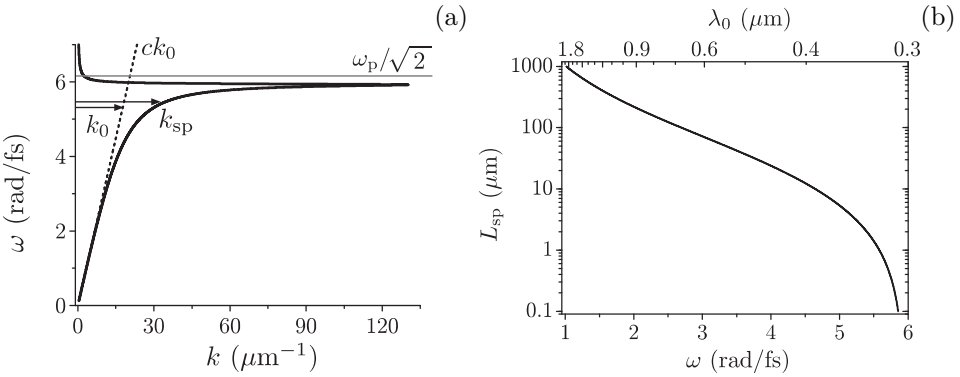

Figure 1.2. (a) Dispersion of the surface plasmon on the sodium-vacuum interface (solid black line). The dashed line shows the light line ($\omega = ck_0$). Arrows show that the SP wavenumber k_{sp} exceeds the free radiation wavenumber k_0. (b) Surface plasmon propagation length L_{sp} on the sodium-air interface.

1.2.2 Surface plasmon dispersion and attenuation

The dispersion of the surface plasmon, i.e., the dependence of the SP frequency ω on its wave number k_{sp} shows how the properties of the surface plasmon change in various frequency ranges, and determines the value of both the phase and group velocities. To gain a conceptional understanding of the dispersive properties of a surface plasmon we return to the Drude model (see Eq.(1.2)) for the dielectric function of the metal, and assume the dielectric to be dispersionless. Metallic sodium behaves very much like a Drude metal, i.e., the dispersion of its dielectric function can accurately be fitted with the Drude model yielding $\omega_p = 8.7$ rad/fs and $\gamma = 0.042$ fs^{-1} [18]. The results for the SP dispersion and the damping on the sodium-vacuum interface are shown in Fig. 1.2.

At low frequencies (near IR and IR, $\omega < 2$ rad/fs) the SP on the Na-vacuum interface has a photon-like nature, i.e., its phase velocity is very close to the speed of light: it extends mainly in the vacuum rather than in the metal. At optical frequencies the dispersion curve $\omega(k_{sp})$ starts to bend over, which results in a decrease of the SP group velocity $v_{gr} = \partial\omega/\partial k_{sp}$ and higher damping due to deeper penetration of the SP into the metal. In the limit that $\omega \to \omega_p/\sqrt{2}$ the SP becomes a localized excitation, since $v_{gr} \to 0$. At the largest value of k_{sp} ($k_{sp} \sim 130$ μm^{-1}) the dispersion curve is seen to fold back. Along this branch the group velocity is negative, a notion that has spawned quite a few papers [19–21]. In this spectral region the SP is, however, so

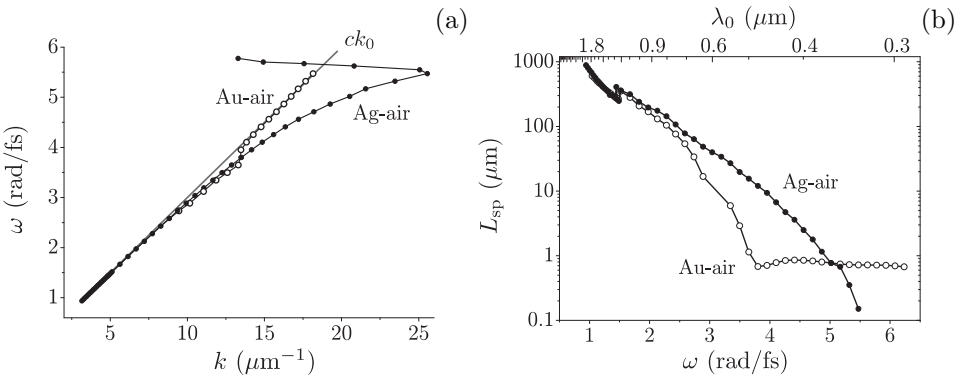

Figure 1.3. The dispersion (a) and damping (b) of a surface plasmon on gold-air (○) and silver-air (●) interfaces. Data are based on tabulated values for the dielectric functions of metals [22].

strongly damped that the concept of a propagating wave loses its meaning.

Figure 1.2b shows how the attenuation length L_{sp} varies as a function of the frequency of the surface plasmon. While for frequencies $\omega < 4.7$ rad/fs the relationship between L_{sp} and ω is almost exponential, for higher frequencies L_{sp} drops even much more rapidly.

In most practical cases it is convenient to use metals that are less reactive than sodium, e.g. gold or silver. The dispersion and damping of a surface plasmon on a gold-air or silver-air interfaces are shown in Fig. 1.3. Clearly, silver behaves much better than gold insofar that the wavenumber of the surface plasmon on the silver-air interface deviates much more from the light line than on the gold-air interface. Additionally silver shows a lower SP attenuation compared to gold. However, gold doesn't oxidize in air, which makes it easy to study surface plasmons on the gold-air interface while thin silver layers are prone to chemical attack in air [23]. Note that it is still possible to study SPs on the silver-dielectric interface when the silver layer is buried or freshly applied.

1.2.3 Surface-plasmon excitation

The value of the SP wave number k_{sp} is larger than that of light in free space k_0 (see Fig. 1.2a). Consequently, there is a wave-vector mismatch between the surface plasmon and free-space radiation, and it is therefore not possible to directly excite the SP by shining light on a smooth metal surface [8]. Various schemes have been used [24] to add the missing momentum to the incident photon (see Fig. 1.4). Prism coupling schemes, shown in Fig. 1.4a–c, as pro-

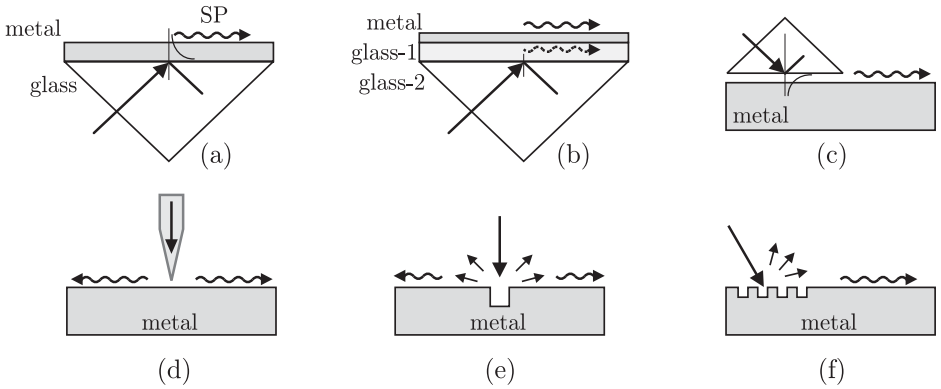

Figure 1.4. Surface-plasmon excitation schemes: a) Kretschmann configuration; b) double-layer Kretschmann configuration; c) Otto configuration; d) excitation with a SNOM probe; e) light diffraction on a single surface feature; f) excitation by means of a diffraction grating.

posed by Kretschmann and Otto [25, 26], are still widely used, especially in surface-plasmon spectroscopy [27, 28]. These schemes require careful angular tuning of the setup to couple to the surface plasmons. A scanning near-field optical microscope (SNOM) tip (Fig. 1.4d) is also a widely used powerful tool for both local excitation and probing of the surface plasmons [29–33]. Finally, a surface feature like a protrusion, grating, or surface roughness can be employed to excite and de-excite SPs (Fig. 1.4e–f). In all cases the polarization of the incident radiation has to be chosen so as to optimally couple with a surface plasmon. In the present thesis, where we use one, two or three slits to launch and detect surface plasmons, the incident light has to be polarized perpendicular to the slit axis.

Obviously, the detailed shape of the surface feature has a major impact on the excitation probability of a surface plasmon. Naively, one can say that for normally incident light the excitation probability is determined by the square of the Fourier transform of the surface feature at the wave vector of the surface plasmon. For a rectangular bump of width a the Fourier spectrum is shown in Fig. 1.5. It is seen to rapidly drop off and to become zero when $k = 2\pi/a$. This suggests that, in order to efficiently excite surface plasmons one should have $k_{\mathrm{sp}} \ll 2\pi/a$, i.e. $a \ll \lambda$. In that case the SP excitation probability only weakly depends on λ.

In the work described in this thesis sub-wavelength slits are employed as both source and probe of surface plasmons [34, 35], the main reason being the simplicity of the structure and the intuitiveness of the physics. As an example,

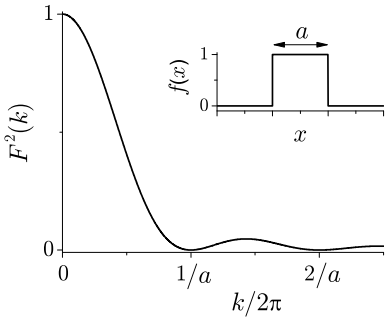

Figure 1.5. Fourier spectrum of a step function.

one of the studied structures is shown in Fig. 1.6 together with the light pattern behind it, observed under two illumination conditions. The sample is a 200 nm thick gold film, deposited on top of 0.5 mm thick glass plate with a 10 nm Ti adhesion layer between the gold and the glass. The gold film is perforated by two parallel, 0.2 μm wide and 50 μm long slits, that are 25 μm apart. One of the two slits is illuminated by a tightly focused laser beam with a spot size of order 5 μm, much smaller than the slit separation. The laser is tuned to a wavelength of 800 nm where the SP on the Au-air interface is weakly damped ($L_{\mathrm{sp}} \simeq 90$ μm). The polarization of light can be chosen to be either TE or TM, i.e. parallel or perpendicular to the length of the slits. The dark side of the sample is imaged on a CCD camera by means of a microscope objective (40/0.65). Figures 1.6b and c show the case for TE and TM illumination, respectively. Under TM illumination the non-illuminated slit is bright being "fed" by the SP launched by the illuminated slit at left.

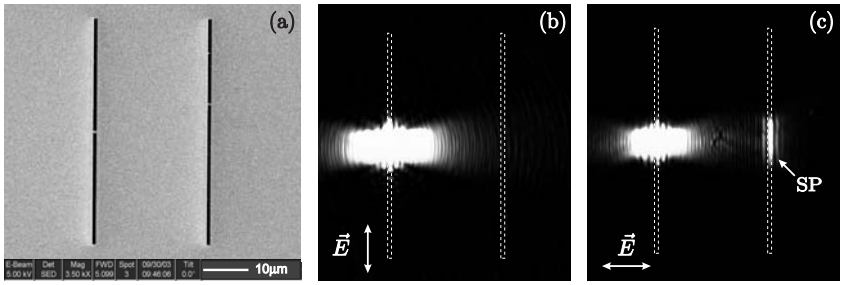

Figure 1.6. (a) SEM image of the sample; (b) Source slit is illuminated with TE polarized light and probe slit remains dark as surface plasmons are not excited; c) Source slit is illuminated with TM polarized light and probe slit becomes bright, scattering the incident SP to propagating light. The positions of the slits are indicated by dashed lines.

1.3 Outline of thesis

The work in this thesis describes a series of interlinked experiments on surface plasmons propagating along a metallo-dielectric interface. The metal is either gold or silver applied as a thin ($\approx$ 200 nm thick) film on top of a transparent substrate with a binding layer in between. That film is perforated by a number of long, sub-wavelength slits, separated by many optical wavelengths (see Fig. 1.6). The common idea behind all the experiments is that each of the slits has a number of functions:

1. It transmits part of the incident light.
2. It scatters part of the incident light into a surface plasmon that propagates along the interface.
3. It scatters part of an incident surface plasmon into light, being visible at both the front and rear sides of the sample.

This list is not complete; however, it enumerates the effects that dominate the experimental results described in this thesis.

In the second Chapter we study a sample consisting of a 200 nm thick gold film on top of a glass substrate with a titanium adhesion layer between the gold and the glass. The metal film is perforated by a series of double slits, each of the slits being $\approx$ 50 μm long and 200 nm wide. There are five sets of double slits, each with a different inter-slit distance, namely 5, 10, 15, 20 and 25 μm. When illuminated by a spatially coherent, narrow-band source, each slit pair will give rise to the well-known double-slit interference pattern, described in any textbook on optics or wave phenomena. Here we do not study this well-known interference phenomenon; instead we look at the *total* amount of light transmitted by the double slit. We vary the wavelength of the incident light and observe a periodic modulation of the transmitted power, the modulation period being inversely proportional to the slit separation. The visibility of this interference phenomenon is strongly affected by the slit width so that the effect is most pronounced when very narrow slits are used. We attribute this modulation to an interference effect, namely between light directly transmitted by one of the slits and light that transiently traveled as a surface plasmon, having been launched by the other slit. The slits experience cross talk due to the surface plasmons.

We have included some experiments on a 200 nm thick titanium film, a material that exhibits extremely strong surface-plasmon damping. This sample does not exhibit any spectral modulation of the transmittivity, in line with our description in terms of surface-plasmon cross talk. Similarly, the

spectral modulation is also not observed if the incident light is TE-polarized, i.e., is polarized parallel to the slits.

In Chapter 3 we use the same configuration as in Chapter 2 but we focus the incident radiation on just *one* slit. When looking at the unilluminated side of the sample one observes that *both* slits transmit light, one much stronger than the other (the non-irradiated slit). In this second system exhibiting plasmonic cross talk we study the nature of the far-field interference pattern, specifically how the interference orders move when the wavelength of the incident radiation is changed. In a second experiment, we illuminate both slits, the light incident on slit 1 being totally incoherent with the light incident on slit 2. Nevertheless, the far field behind the double slit shows clear interference features indicating that the light exiting the slit is in part *coherent*. Here the cross-coupling due to the surface plasmons acts as a source of coherence.

The spectral fringes that one observes in the experiment described in Chapter 2 are slightly non-sinusoidal, indicating that the effect is possibly more than a two-beam interference effect. That suggests a picture of a resonator, with the surface plasmon bouncing between mirrors, in our case the slits. In Chapter 4 we explore this picture of a bouncing surface plasmon using a time-domain approach. In this Chapter we use pairs of slits separated by 25, 50, 75 or 90 μm. We are able to observe the surface plasmon making two full round trips through the cavity. This experiment allows us to determine the surface-plasmon power reflection coefficient, obtain information on the phase shift in various scattering processes, and directly measure the surface-plasmon group velocity at the wavelength of the incident radiation.

In Chapter 5 we use a sample containing not two but three slits, two of which are parallel, the third one intersecting the other two at a rather acute angle. The surface plasmons now give rise to an intricate interference pattern in each of the slits unless the polarization of the incident radiation is chosen so that a specific slit does not directly transmit the incident light or does not launch surface plasmons. By judiciously selecting the polarization of the incident light and the dimensions of the sample we are able to observe the standing surface-plasmon wave launched by the two parallel slits. By comparing the light transmitted by various parts of the structure we are able to obtain information on the scattering phase acquired when light is scattered into a plasmon an back-scattered into light, and on the amplitude and phase acquired by the surface plasmon as it "transits" a sub-wavelength slit.

The experimental study of the structures studied in Chapters 2 and 3 brought to light that our sub-wavelength slits milled through our thin metal layers are much less polarization selective (in terms of their direct transmis-

sion) than one would naively think. Moreover, when the incident light is linearly polarized at an angle of 45° relative to the slit the transmitted light is circularly polarized, indicating that such a slit is highly birefringent.

However, it is widely assumed that a slit with width $\approx \lambda/4$ has a very much smaller transmission for incident light that is TE-polarized as compared to light that is TM-polarized and our initial results were therefore quite puzzling. In Chapter 6 we investigate this by studying the width dependence of the transmission of a single slit. We compare our experimental data with the results of a numerical calculation and obtain excellent agreement. The strong birefringence of certain slits is explained in terms of the difference in phase evolution between a propagating and an evanescent mode.

In Chapter 7 we apply the spectral modulation method of Chapter 2 to the study of surface-plasmons propagating along a buried interface, namely the silver-glass interface. From a plasmonic point of view, silver is much to be preferred over gold being a much less lossy metal, particularly at higher photon energies (in the blue spectral region). However, silver has a disadvantage in that it rapidly tarnishes in air, requiring the plasmon-supporting interface to be buried. There are two interesting aspects to studying surface plasmons on such a buried interface: the surface-plasmon wavelength $\lambda_{\mathrm{sp}} = 2\pi/k_{\mathrm{sp}}$ is reduced by, roughly, the refractive index of the dielectric n_{d}, and the damping is increased by a factor of order n_{d}^3. On this sample we are able to observe plasmonic interference up to photon energies of 2.6 eV (vacuum wavelength $\lambda_0 = 477$ nm), corresponding to a plasmonic wavelength of 260 nm, one of the shortest reported values to date.